WATER RESEARCH 56 (2014) 314–324

Available online at www.sciencedirect.com

ScienceDirect

journal homepage: www.elsevier.com/locate/watres

Fate of hydrolyzed Al species in humic acid coagulation

Jr-Lin Lin [a], *Chihpin Huang* [a,*], *Brian Dempsey* [b], *Jing-Yi Hu* [a]

[a] *Institute of Environmental Engineering, National Chiao Tung University, Hsinchu, Taiwan*
[b] *Department of Civil and Environmental Engineering, Pennsylvania State University, University Park, PA 16802, USA*

ARTICLE INFO

Article history:
Received 8 November 2013
Received in revised form
29 January 2014
Accepted 1 March 2014
Available online 12 March 2014

Keywords:
Coagulation
PACl
Al_{13}
Humic acid
Organic matter

ABSTRACT

The hydrolysis of Al-based coagulants in acidic conditions is necessary for the removal of organic matter by the coagulation/sedimentation process. However, interactions between hydrolyzed Al species and organic matter are complicated and this makes it difficult to optimize coagulant dosing for organics removal. The goal of this study was to investigate the reactions of hydrolyzed Al species in the coagulation of organic matter. Two polyaluminum chloride (PACl) coagulants, a commercial product with sulfate (PACl-C) and lab-prepared material (PACl-Al_{13}) containing 7% and 96% of total Al as Al_{13}, respectively, have been applied to investigate the coagulation of humic acid (HA). At pH 6, a lower dosage of PACl-Al_{13} than of PACl-C was required for optimized HA removal through coagulation/sedimentation due to the strong complexation and charge neutralization by Al_{13}. Observation of the coagulation process using wet scanning electron microscopy showed that PACl-C produced both clustered flocs and linear precipitates in the presence of sulfate while PACl-Al_{13} produced curled precipitates due to the formation of intermolecular complex, when both coagulants were added at the optimum doses. Investigation of Al–HA floc by ^{27}Al-NMR and Al 2p XPS suggested that monomeric Al (Al_m) was hydrolyzed into $Al(OH)_3$ with tetrahedron for PACl-C coagulation while a half of Al_{13} slowly decomposed into octahedral Al–HA precipitates for PACl-Al_{13} coagulation. Meanwhile, C ls XPS indicated that aromatic C=C of HA was preferentially removed from solution to Al–HA flocs for both PACl-C and PACl-Al_{13} coagulation. It was concluded that Al–HA complexation strongly affects the reaction pathways for Al hydrolysis and the final nature of the precipitates during PACl coagulation of HA and that the hydrolysis products are also strongly affected by the characteristics of the PACl coagulant.

* *Corresponding author*. Tel.: +886 3 5712121x55507; fax: +886 3 5725958.
E-mail address: cphuang@mail.nctu.edu.tw (C. Huang).

http://dx.doi.org/10.1016/j.watres.2014.03.004
0043-1354/

1. Introduction

Humic substances (HS) are colored and generally represent more than 50% of dissolved organic matter (DOM) in surface waters (Alborzfar et al., 1998). Many problems are associated with HS in the context of drinking water quality, including undesirable color, tastes and odors, and particularly the occurrence of carcinogenic disinfection-by-product (DBP) during chlorination (Gallard and Gunten, 2002).

In most surface waters, aquatic fulvic acid is the major component of HS, but humic acid (HA) is also present simultaneously (Edzwald and Tobiason, 1999). In water treatment, HA removal is mainly achieved by coagulation with hydrolyzed metal species (Duan and Gregory, 2003). HA removal by using various coagulants has been widely explored to determine the optimum condition for HA destabilization (Exall and Vanloon, 2000; Sieliechi et al., 2008). These studies have suggested that the optimum condition of coagulation for HA removal is closely related to pH due to effects on hydrolyzed metal species, which subsequently affect the degree of HA destabilization. The mechanisms of HA destabilization by hydrolyzed coagulant species have been well established. A combination of complexation of HA with metal ions, adsorption onto metal hydroxide precipitates, and co-precipitation with metal hydroxides are important in HA removal (Dempsey et al., 1984; Huang and Shiu, 1996).

Polyaluminum chloride (PACl) has been commonly adopted to remove organic matter by coagulation in water practices. The nature of PACl coagulant is highly related to its basicity (γ), which strongly affects the coagulation behavior. Some investigators have suggested that the basicity adjusted in the range from 2 to 2.3 during the preparation of PACl can produce high content of Al_{13} polycation (i.e., $[AlO_4Al_{12}(OH)_{24}(H_2O)_{12}]^{7+}$) (Bottero et al., 1980; Van Benschoten and Edzwald, 1990; Shen and Dempsey, 1998). Study has indicated that the major pre-hydrolyzed species of PACl is Al_{13} polycation that can subsequently destabilize HA by strong charge neutralization to effectively remove HA from water through coagulation/sedimentation process (Liu et al., 2009). However, other studies have reported that *in-situ* hydrolyzed Al_{13} shows better performance in the removal of natural organic matter (NOM) by coagulation/sedimentation (Hu et al., 2006; Zhao et al., 2008). In the presence of NOM, the Al_{13} polycation is converted into monomers catalyzed by complexation with organic ligands (Masion et al., 2000; Yamaguchi et al., 2004), and this could affect the efficiency of HA removal by PACl coagulation. The characteristics of HA and hydrolyzed metals floc governs floc density and settling rates, which dictates the efficiency of HA removal. Wang et al. (2007) have indicated that the HA flocs formed by PACl coagulation are multi-scale fractal, and their surface characteristics, such as irregularity and roughness, vary with the ratio of coagulant dosage and the quantity of HA. This implies that the structure of HA flocs could be significantly affected by Al–HA interaction. Kazpard et al. (2006) has suggested that the optimal coagulant dosage is a function of the interactions between the functional groups of HA and Al_{13} polycation. Although these studies have investigated the effect of PACl coagulation on the efficiency of HA removal through investigation into Al–HA interactions, the interaction mechanisms of hydrolyzed Al species and HA remains unclear because the pathway of Al species hydrolysis and decomposition in the presence of HA are complicated and may depend on coagulation conditions such as pH and dosage. In other words, the fate of hydrolyzed Al species in HA coagulation is the key factor to optimize HA destabilization, but it is still not fully understood.

In this study, the effect of Al species on the coagulation performance of humic acid (HA) was evaluated and the chemical interactions between hydrolyzed Al and HA were investigated. Two polyaluminum chloride (PACl) coagulants, one commercial PACl (termed PACl-C) and another custom-made PACl (designated PACl-Al_{13}) containing Al_{13} with 7% and 96% of total Al concentration, respectively, were mixed with HA in water. The Al–HA flocs that formed after coagulation at various pH values were investigated by X-ray photoelectron spectroscopy (XPS) and solid-state ^{27}Al nuclear magnetic resonance (^{27}Al NMR) to verify the nature of the reaction products and to identify the reaction mechanisms between HA and Al species. The morphology of Al–HA flocs was also examined by wet scanning electron microscopy (WSEM).

2. Materials and methods

2.1. Humic acids solution

A synthetic humic acid powder (Aldrich Co., USA) was added into distilled (DI) water and the solution was adjusted to pH 1 using HCl. After 10 min settling, the solution was centrifuged for 20 min and then the supernatant was withdrawn into DI water. After that, the solution was stirred at pH 11 by NaOH to completely hydrate and dissolve the remaining HA, followed by the filtration through 0.45-μm membrane. The filtrate was used as a synthetic stock solution, to which DI water was added to prepare the experimental HA solutions at the desired concentration of 5 mg/L. The specific conductivity of the working suspension was adjusted with 10^{-3} M $NaClO_4$ solution (Merck, Inc., USA) and the alkalinity was adjusted by adding 10^{-3} M Na_2CO_3 (Merck, Inc., USA). The conductivity and alkalinity of HA suspension is 357 μs/cm and 105 mg/L as $CaCO_3$, respectively.

2.2. Characterization of coagulants

Study reported that the content of Al_{13} polycation varies with the basicity in the preparation of PACl, and the PACl containing higher content of Al_{13} is more efficient to destabilize the organic matter by charge neutralization during coagulation (Liu et al., 2009). To investigate the effect of hydrolyzed Al species on the HA coagulation, two PACl coagulants with different basicity were used to evaluate the performance of coagulation in this study. A commercial-grade PACl (Al_2O_3 = 10%; γ = 1.4) was purchased from Showa Chemicals Inc., which was designated as PACl-C herein. Another PACl identified herein as PACl-Al_{13} contained high Al_{13} content that was separated from preformed PACl (Al_2O_3 = 29%; γ = 2.3) by sulfate precipitation and nitrate metathesis (SO_4^{2-}/Ba^{2+} separation method) (Shi et al., 2007). Based on the results of sulfate analysis by Ion Chromatography (833 Basic IC plus, Metrohm,

Switzerland), the content of sulfate ions in the PACl-C coagulant is about 1.96% and the sulfate ions do not exist in the PACl-Al_{13} coagulant. The working solutions containing 1000 mg/L Al were freshly prepared before each test. Aluminum concentration was analyzed by an inductively coupled plasma atomic emission spectrometry (ICPAES, JY24, Jobin-Yvon Inc., France).

The Al speciation of PACl and PACl-Al_{13} was determined by ferron assay and ^{27}Al-NMR test (Uniytinova-500, Varian, USA). A ferron assay was carried out for the quantitative analysis of the Al species (Lin et al., 2009). On the basis of the kinetics of the reaction between the Al species and the ferron reagent, the hydrolyzed Al species could be categorized into three types: monomeric Al (Al_a), polymeric Al (Al_b), and colloidal Al(Al_c). The absorbance recorded in the first minute and that recorded between 1 min and 2 h were assigned to Al_a and Al_b, respectively. The absorbance due to Al_c was obtained by subtracting the absorbances of Al_a and Al_b from the total absorbance. The Al species were quantified by the timed absorbances recorded at 366 nm using a UV–visible spectrometer (U3010, Hitachi Inc., Japan). The total Al concentration of the solution was maintained at 3.7×10^{-4} M Al during the ferron assay. The operation parameters for the NMR analysis were spectrometer frequency, solvent, and temperature, which were 130.24 MHz, D_2O, and 298 K, respectively. A 5-mm sample tube (Wilmad 507-pp, SP Industries Inc., USA) containing 3 mL 0.1 M Al solution and a 4.2-mm sample tube (Wilmad WGS-5BL, SP Industries Inc., USA) containing 1 mL 0.05 M $Al(OD)^{4-}$ solution were co-inserted as the inner standard. The chemical shift of $Al(OD)^{4-}$ was at 80 ppm. The signals in the proximity of 0 and around 62.5 ppm represent monomeric Al (Al_m) and tridecamer Al_{13}, respectively. The concentration of each species was determined by the ratio of the integrated intensity of the corresponding peak to that of $Al(OD)^{4-}$ at 80 ppm. The amount of the undetectable species (denoted as Al_u) was obtained by subtracting the sum of the detected Al species from the total Al concentration. Investigation of Al species in PACl-C and PACl-Al_{13} by both ferron assay and ^{27}Al-NMR test showed that the PACl-C contained about 40% monomeric Al (Al_a) and 50% colloidal $Al(OH)_3$(Al_c), while the PACl-Al_{13} contained more than 95% Al_{13}(Al_b), with more than 95% of total Al concentration, as presented in Table 1.

2.3. Coagulation protocol

Standard jar trials were conducted to evaluate coagulation performance. Each jar trial was conducted at the desire pH condition after rapid mixing by adding HCl or NaOH before coagulation. The rapid mixing was conducted at 200 rpm ($G = 350\ s^{-1}$) for 1 min followed by a slow mixing at 30 rpm ($G = 25\ s^{-1}$) for 15 min. The suspension was left undisturbed for 20 min. After settling, the supernatant was immediately filtered through a 0.45 μm glass fiber paper, and then the residual dissolved organic carbon (DOC) of filtrate was quantified by TOC analyzer (TOC-5000A, Shimadzu, Japan). The zeta potentials (ZP) of the suspension were measured via a laser zeta analyzer (Zetasizer nano ZS, Malvern Inc., UK) immediately after the rapid mixing without dilution. The median diameter (d_{50}) of flocs formed after slow mixing was determined by a particle size analyzer (Mastersizer 2000, Malvern Inc., UK). All coagulant dosages used in this study were in mg/L as Al.

2.4. Solid-state ^{27}Al magic-angle spinning nuclear magnetic resonance

The solid-state magic-angle spinning nuclear magnetic resonance (MAS-NMR) spectra were recorded by a Bruker instrument (DSX-400WB, Bruker, Germany) in 4 mm rotors, and the ^{27}Al spectra were recorded at 104.1 MHz. The solid-state ^{27}Al MAS-NMR was performed on freeze-dried PACl-C and PACl-Al_{13} aggregate samples from experiments at various dosages. The PACl-C and PACl-Al_{13} aggregates formed after coagulation were withdrawn immediately from the suspensions to the plate and then freeze dried over 24 h with a vacuum refrigerating instrument (FD2-D, Kingmech Co., Ltd, Taiwan).

2.5. Wet scanning electron microscope (WSEM)

Aggregates formed after PACl-C and PACl-Al_{13} coagulation were withdrawn into a sealed specimen capsule (QX-102, Quantomix Co. Ltd, Israel) and were protected from vacuum in the microscope by an electron-transparent partition membrane. Therefore, imaging by this way can make the micron-scale observation of fully hydrated samples or water solution maintained at atmospheric pressure. After the placement of samples, the morphology of the wet aggregates was observed by a conventional scanning electron microscope (SEM) (5136LS, Tescan, Czech).

2.6. X-ray photoelectron spectroscopy

XPS was used to determine the surface Al species of PACl-C and PACl-Al_{13} flocs up to depths of less than 10 nm. XPS analysis was performed on an X-ray photoelectron spectrometer (ESCALAB 250, Thermo VG Scientific, UK) using a monochromatized Kα X-ray beam at 3.8 kW generated from a rotating Al anode. All samples were stored in a nitrogen atmosphere to prevent atmospheric contamination and oxidation. Each analysis was commenced with a survey scan in the binding energy range of 0–1000 eV with steps of 1 eV. The binding energies of the photoelectrons were calibrated using the aliphatic adventitious hydrocarbon C(1s) peak at 284.6 eV.

Table 1 – Characteristics of coagulants by Ferron assay and ^{27}Al-NMR method.

Coagulants	γ	pH	Ferron assay (Al %)			^{27}Al-NMR (Al %)		
			Al_a	Al_b	Al_c	Al_m	Al_{13}	Al_u
PACl-C	1.4	3.80	42.3	8	49.7	38.4	6.8	54.8
PACl-Al_{13}	–	4.72	3.7	96.3	0	0	95.8	4.2

3. Results and discussion

3.1. Performance of HA coagulation

The pH condition is a key parameter controlling the effectiveness of coagulation/sedimentation for the removal of organic matter (Duan and Gregory, 2003). In order to understand the pH effect on HA destabilization by PACl coagulation, the performance of coagulation by PACl-C and PACl-Al_{13} were determined at a fixed coagulant dosage of 2.5 mg/L as Al and various pH conditions. The changes of residual DOC along with zeta potentials at various pH values are shown in Fig. 1. The optimum condition for DOC removal by either PACl-C or PACl-Al_{13} coagulation occurred at slightly acidic pH where the zeta potentials were increasing with decreasing pH, consistent with earlier studies showing that the optimum HA destabilization occurs at acidic pH (O'Melia et al., 1999). By contrast, the residual DOC increased sharply when pH was higher than 6 for which the zeta potential was extremely negative, resulting in poor HA destabilization.

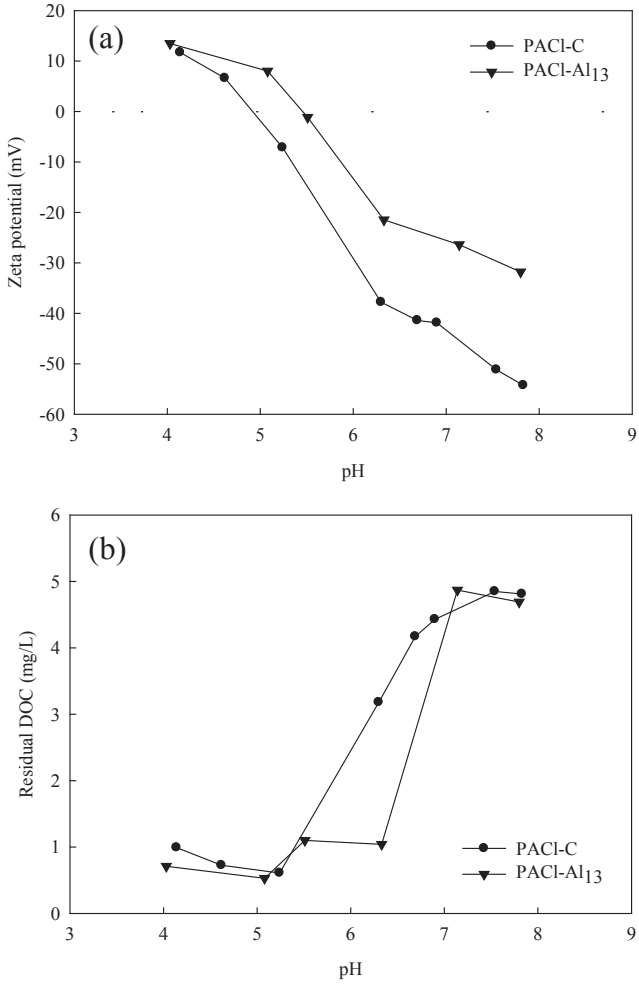

Fig. 1 – DOC removal varies with pH for PACl-C and PACl-Al_{13} coagulation (a) zeta potential (b) residual DOC (initial DOC: 5 mg/L; dosage: 2.5 mg/L as Al).

Studies have suggested that the predominant mechanism for organic matter coagulation/sedimentation is dictated by the nature of the hydrolyzed Al species, such as Al_{13} aggregates and $Al(OH)_3$ precipitates (Hu et al., 2006; Zhao et al., 2008). Lin et al. (2008a) suggested that Al_{13} is fairly stable at slightly acidic pH but preferentially aggregates into larger clusters due to inter-particle bridging when the pH exceeds 7, while monomeric Al transforms into Al_{13} *in-situ* and eventually forms $Al(OH)_3$ precipitates at neutral pH. It is likely that particle destabilization occurs either by charge neutralization at lower doses or by sweep floc at higher doses. The predominant mechanism of HA destabilization at slightly acidic pH is charge neutralization (Dempsey et al., 1984). Charge neutralization is most effective with increasing positive charge on hydrolyzed Al species and decreasing negative charge on HA, and therefore the lowest effective coagulant doses are typically observed with slightly acidic pH conditions. Related, DOC removal by PACl-Al_{13} coagulation is superior to that by PACl-C coagulation at slightly acidic condition (around pH 6).

However, the coagulation mechanism by hydrolyzed Al species is also governed by the dosage of coagulant (Lin et al., 2009) and this also influences the removal efficiency of organic matter. To verify this, coagulation trials with various dosages were conducted at pH 6 and the residual DOC and zeta potentials were determined for PACl-C and PACl-Al_{13}. The results are illustrated in Fig. 2. For PACl-C coagulation, good removal occurred with 4 mg/L Al consistent with charge neutralization (zeta potential was zero) and the best DOC removal occurred using 6 mg/L of Al where the positive zeta potential, indicating the removal mechanism included sweep flocculation. For PACl-Al_{13} coagulation, effective coagulation was achieved at a lower dosage of 2.5 mg/L Al where the zeta potential was still negative. These results indicate that the predominant mechanisms for HA destabilization by PACl-C and PACl-Al_{13} coagulation were markedly different. Because the properties of the floc surfaces are significantly affected by Al–HA interactions (Xu et al., 2012), the following studies were carried out to observe the morphology and chemical characteristics of PACl-C and PACl-Al_{13} flocs and the associated HA in order to further clarify mechanisms for HA removal when using PACl-C or PACl-Al_{13}.

3.2. Morphology of Al–HA floc

To observe the hydrated structure of Al–HA flocs, the WSEM was used to image the morphology of various Al–HA flocs *in-situ* in a liquid environment. The WSEM images of Al–HA flocs coagulated by PACl-C and PACl-Al_{13} at optimum dosage (i.e., 2.5 mg/L Al and 6 mg/L Al, respectively) are shown in Fig. 3. There are marked differences between the morphology of PACl-C and PACl-Al_{13} flocs. In addition, the evidence showed that PACl-C flocs (d_{50} = 252 μm) are larger than PACl-Al_{13} flocs (d_{50} = 210 μm). For PACl-C coagulation, larger precipitates had either linear needle-like shape or more massive and irregular dimensions, as shown in Fig. 3 (a). Based on extensive liquid-state and solid-state ^{27}Al NMR, Lu et al. (1999) suggested that HA assumed a particular adsorbed structure that partially covered the surface of $Al(OH)_3$ precipitates when the pH exceeded 5. In addition, our previous research has suggested

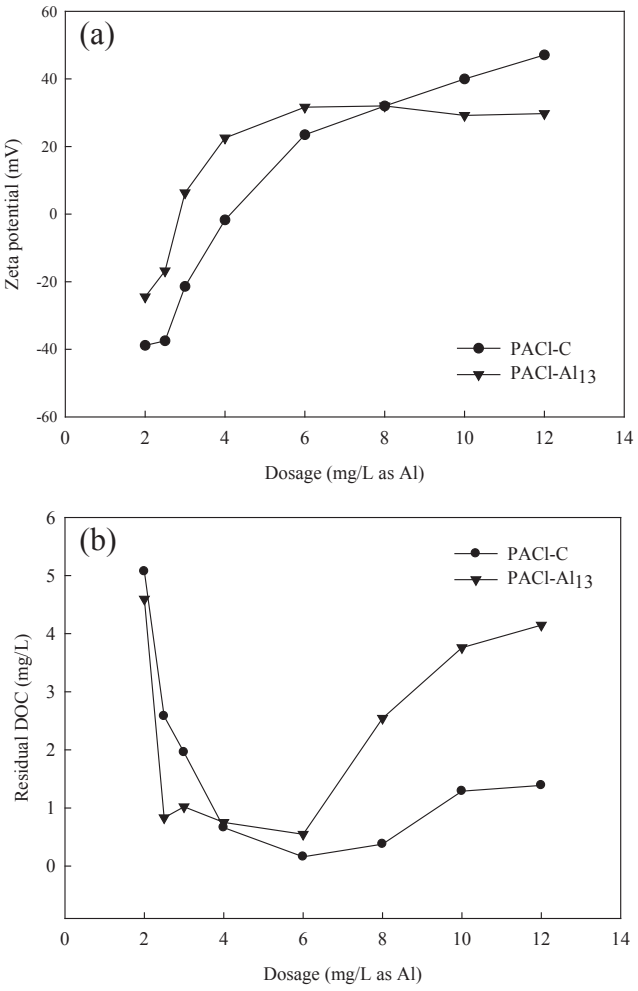

Fig. 2 – DOC removal varies with dosage for PACl-C and PACl-Al_{13} coagulation (a) zeta potential (b) residual DOC (initial DOC: 5 mg/L; final pH: 6).

that there are large amounts of $Al(OH)_3$ colloids with micro-scale structure in PACl-C coagulation (Lin et al., 2008b). These studies indicated that the surfaces of colloidal $Al(OH)_3$ precipitates using optimum low doses of PACl-C at pH 6 could be covered with HA. In this study, sweep flocculation dominated the aggregation for PACl-C coagulation at the dosage of 6 mg/L Al, while the optimum HA aggregation was induced by charge neutralization for PACl-Al_{13} coagulation at the dosage of 2.5 mg/L Al, as illustrated in Fig. 2. As shown in Fig 3 (a), the needle-like and globular shapes were interpreted to be possibly due to the formation of positively-charged Al–HA complex and the occurrence of $Al(OH)_3$–HA cluster during PACl-C coagulation, respectively. Because a few sulfate ions remained in the PACl-C coagulant (SO_4^{2-}/Al = 0.37), these sulfate ions promoted the polymerization of monomers and the precipitation of colloidal $Al(OH)_3$ (Wang et al., 2002). In part, the positively-charged Al (e.g. monomeric Al) could complex with SO_4^{2-} to enhance the aggregation of negatively-charged supramolecular HA by intermolecular bridging during coagulation (Wu et al., 2012). However, these positively-charged Al with weak charge neutralization ability could not strongly destabilize HA to form cluster due to complexation between SO_4^{2-} and Al. As a result, a low quantity of linear precipitates was found. In addition, the majority of $Al(OH)_3$ colloids formed during PACl-C coagulation could be partially covered with HA or Al–HA complex in the initial stage of coagulation, and then the clustered precipitates with globular structure could be formed eventually by enmeshment.

By contrast, the PACl-Al_{13} flocs are smaller with a curled structure. During PACl-Al_{13} coagulation, the nano-scale stereo Al_{13} (Keggin structure) with many positively-charged binding sites was easily adsorbed onto HA, and then formed the micro-scale Al_{13}–HA aggregates either by charge neutralization or intermolecular complex between Al_{13} and HA. Consequentially, the curled flocs were observed in Fig 3 (b). However, the decomposition of Al_{13} in Al_{13}–HA complexation process could indirectly cause the formation of $Al(OH)_3$–HA flocs, which results in the occurrence of micro-scale PACl-Al_{13} flocs. The images of Al–HA flocs implied that the formation of Al–HA floc varies with hydrolyzed Al species in PACl coagulation. Therefore, surface Al speciation and carbon binding of Al–HA floc was surveyed in the following experiments to explore the interactions between hydrolyzed Al species and HA.

3.3. *Interaction of hydrolyzed Al–HA*

The solid-state ^{27}Al-NMR was used to analyze the hydrolyzed Al species in the Al–HA flocs to understand the predominant Al species that were responsible for removal of HA for PACl-C versus PACl-Al_{13} coagulation. The solid-state ^{27}Al-NMR signals of two coagulated flocs formed at the optimum dosages are shown in Fig. 4. A signal at 0 ppm is typically assigned to octahedral Al, while a signal at 63 ppm is usually assigned to the central tetrahedral Al in the Al_{13} polymer (Bottero et al., 1980). For PACl-C flocs, a strong asymmetric signal occurred at 6.2 ppm and a weak signal was observed at 63 ppm, suggesting that Al was mostly octahedral, either as Al–HA complexes or Al hydroxide precipitates because the PACl-C is initially mostly octahedral (Sposito, 1996). In addition, a weak signal at around 35 ppm indicated the presence of pentahedral Al, which could be produced during the rapid and chaotic formation of amorphous Al hydroxide (Isobe et al., 2003) or could be due to the freeze-drying preparation process (Kazpard et al., 2006). In the case of PACl-Al_{13} flocs, only two strong signals occurred at around 0 and 63 ppm, respectively. The broad signal around 0 ppm suggests that $Al(OH)_3$ or Al-organic ligand complex could form after Al_{13} decomposition induced by organic acid (Ross et al., 2001). This evidence confirms that Al_{13} decomposition occurred during PACl-C and PACl-Al_{13} coagulation for HA destabilization.

The ratio between octahedral and tetrahedral Al on the surfaces of PACl-C and PACl-Al_{13} flocs were determined to further verify the fate of Al species in coagulation. Quantitative analysis of the Al 2p formed on the surfaces of PACl-C and PACl-Al_{13} flocs were carried out by high-resolution XPS, as illustrated in Fig. 5. Two overlapping bands associated with two different Al 2p transitions with binding energies of 72 eV and 74 eV were observed, which corresponded to Al^{IV} and Al^{VI}, respectively (Duong et al., 2005). Changes in the binding energy of surface Al in the XPS pattern could occur due to the

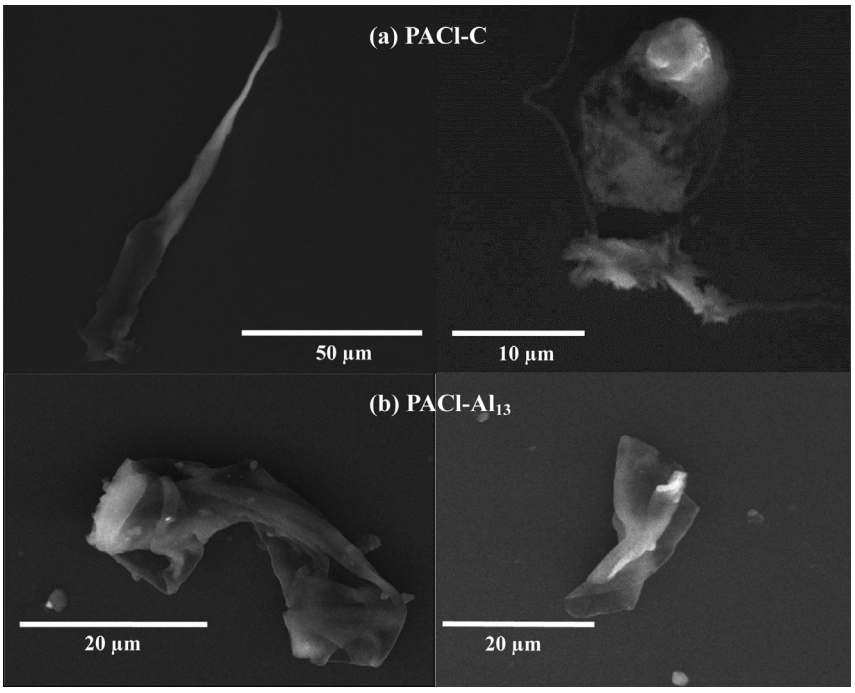

Fig. 3 – WSEM images of flocs formed by PACl-C and PACl-Al_{13} coagulation at optimum dosage (final pH: 6) (a) PACl-C and (b) PACl-Al_{13} flocs

Al–HA complexation. However, one study reported that the binding energy of Al 2p of Al_2O_3 did not change after the formation of an Al_2O_3–HA oxide (Jin et al., 2008). The characteristic peak of octahedral and tetrahedral Al in the XPS survey data of PACl-C and PACl-Al_{13} flocs in the presence of HA, as shown in Fig. 5. There was a small difference in the characteristic peaks of tetrahedral Al in the XPS survey data of PACl-C and PACl-Al_{13} flocs. For PACl-C flocs, the characteristic peak of tetrahedral Al was due at 73 eV, while it was 72.7 eV for PACl-Al_{13} flocs. A shift less than 0.5 eV is within the range of

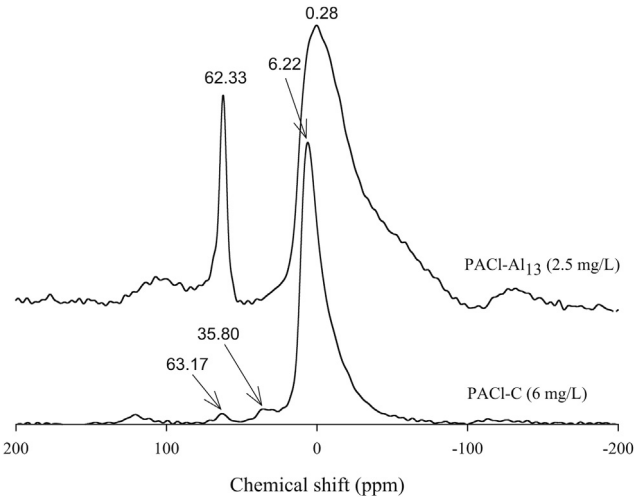

Fig. 4 – Solid-state ^{27}Al NMR spectra of freeze-dried Al-AH floc using PACl-C and PACl-Al_{13} coagulation at the optimum dosage (final pH: 6).

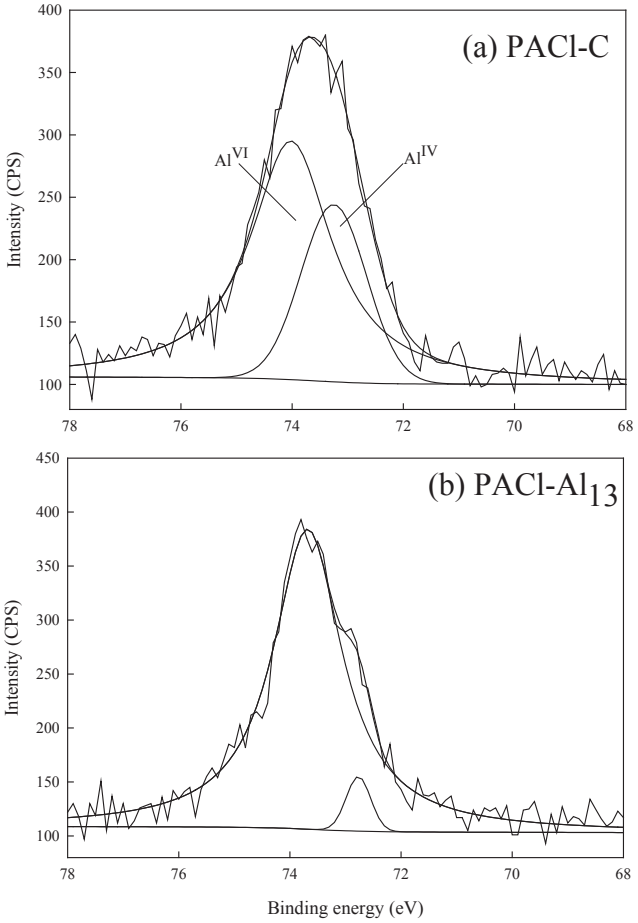

Fig. 5 – Al 2p spectra of XPS (a) PACl-C flocs (b) PACl-Al_{13} flocs

the typical precision of the XPS instrument. As a result, the characteristic peak of octahedral or tetrahedral Al on the surface of PACl-C flocs should not be affected by the complexation of surface Al with HA in our study.

As shown in Fig. 5(a), the Al^{IV}/Al^{VI} ratio of the PACl-C flocs was 1:2.5, suggesting the occurrence of a large amount of tetrahedral Al on the surface of PACl-C flocs. Our previous study indicated that monomeric Al was substantially transformed into the Al^{IV} when PACl-C was used as a coagulant in the absence of organic matter, resulting in an increase in the quantities of Al^{IV} on the surface of flocs (Lin et al., 2009). However, the hydrolysis of Al could be significantly affected by organic ligand for HA coagulation. In theory, the conversion from Al_m to Al_{13} was slower than the formation of Al_m-HA complex (Dempsey, 2006). Thus, Al_m species in PACl-C (around 40% of total Al) could not substantially undergo hydrolysis and transform into Al_{13} after dosing. Although Al_m could partially transform into Al_{13} *in-situ*, the decomposition of *in-situ* hydrolyzed Al_{13} could be caused by Al_{13}-HA complexation (Hiradate and Yamaguchi, 2003; Hu et al., 2006). Theoretically, the Al^{IV}/Al^{VI} ratio in Al_{13} molecules should be approximately 1:12 (Johansson, 1960), but the ratio of Al-IV to Al-VI on PACl-C flocs was 1:2.5, indicating voluminous Al_{13} do not exist in the PACl-C flocs. This phenomenon could be explained by the reaction of Al hydrolysis. Furrer et al. (2002) proved that the various Al species in $Al(OH)_{3(am)}$ flocs in natural rivers originate from the aggregation of the Keggin Al_{13} polycation by the intensive mixing or an episodic reaction in which these polycations probably behave as $Al(O)_4$ centers. In addition, Van Benschoten and Edzwald (1990) concluded that the polymeric structure remains intact within the PACl precipitates. In our study, $Al(OH)_3$-HA precipitates were obviously found in the PACl-C flocs, as shown in Fig 3 (a). Because XPS survey only can provide the information about the content of Al species on the surface of flocs, a large quantity of $Al(OH)_3$ containing tetrahedral Al on the surface of PACl-C flocs could be intensively detected by XPS survey. Based on this hypothesis, a few amount of monomeric Al could be rapidly converted to metastable Al_{13} during the initial stages of PACl-C coagulation in the presence of HA, and Al_{13} formed *in situ* can become converted to $Al(OH)_3$ via the condensation of Al_{13} (Sposito, 1996). In this study, the precipitation of $Al(OH)_3$ was enhanced undergo the hydrolysis of monomeric Al in the presence of sulfate ions, but the tetrahedral Al ($Al(O)_4$) structure was still obviously found in the $Al(OH)_3$ precipitates, as reported by previous study (Duong et al., 2005). Therefore, the result of Al speciation detected by XPS is different from that by ^{27}Al-NMR.

By contrast, a distinct change in the Al^{IV}/Al^{VI} ratio was observed from the XPS survey data of PACl-Al_{13} flocs, as plotted in Fig. 5(b). The Al^{VI}/Al^{IV} ratio in PACl-Al_{13} flocs was about 23. This ratio was about twice higher than the theoretical ratio ($Al^{VI}/Al^{IV} = 12$) in Al_{13} molecules. It suggested that the content of tetrahedral Al decreased and there is about 50% decomposition of Al_{13} due to Al_{13}-HA complexation during PACl-Al_{13} coagulation. In thermodynamic hydrolysis, pre-formed Al_{13} was very stable in the absence of organic matter, but addition of organic ligands can accelerate the dissolution of $A1_{13}$ by complexation. Therefore, the decomposition rate of Al_{13} was closely related to the complexation between Al and organic ligands (Casey, 2006; Thomas et al., 1993). Amirbahman et al. (2000) suggested that the rate of Al_{13} decomposition becomes more rapid when the surface sites of Al_{13} have been occupied by HA favorably through the adsorption and complexation. It was also found that the decomposition rate of Al_{13} increased with increasing COOH/Al ratio and Al_{13} disappeared within 10 min as the molar ratio of COOH/Al exceeded 0.8 in the acidic condition. Based on this conclusion, Al_{13} molecules are supposed to decompose tremendously in this study because the C/Al ratio is higher than 4 at the optimum dosage (i.e., 2.5 mg/L as Al) for PACl-Al_{13} coagulation. However, only about a half of Al_{13} molecules decomposed. This could be explained by Al_{13} aggregation in the complexation between Al and HA. In our study, the formation of Al_{13} aggregates could happen for PACl-Al_{13} coagulation at pH 6 because abundant Al_{13} molecules aggregated into larger molecules (i.e., Al_{13} aggregates) as pH increases more than pH 5 (Zhao et al., 2008). Because the Al_{13} aggregates still remained tetrahedral $Al(O)_4$ structure in an episodic reaction through rapid agitation (Furrer et al., 2002), the surface charge of Al_{13} aggregates was lower than that of Al_{13} for PACl-Al_{13} coagulation (Lin et al., 2008a,b). After Al_{13} aggregation, weakly-charged Al_{13} aggregates could not adsorb HA as much as strongly-charged Al_{13}, alleviating the formation of Al_{13}-HA complex and decomposition rate of Al_{13}. As a result, the Al_{13} aggregates with tetrahedral Al still remained within Al_{13}-HA flocs. It was first found that around a half of Al_{13} was destroyed during HA coagulation by prehydrolyzed Al_{13}.

On the other hand, the characteristics of HA could influence the interaction between hydrolyzed Al and HA. Zhao et al. (2009) suggested that hydrolyzed Al species will preferentially complex with aromatic structure in the DBP precursor, which significantly affects the removal efficiency of DBPs. To further verify the effect of compositions of HA on its destabilization by hydrolyzed Al species, the C 1s spectra of HA powder and flocs were surveyed by XPS, as illustrated in Fig. 6. There are markedly different C 1s peaks between the HA powder and flocs. As shown in Fig. 6(a), four obvious chemical binding signals appeared at 284.5 eV, 285.6 eV, 287.9 eV and 290.9 eV, which are assigned to aromatic carbon (C═C), aliphatic carbon (C–C), ketonic carbon (C═O) and carboxylic carbon (O–C═O), respectively (Monteil-Rivera et al., 2000). However, the dramatic changes in C 1s spectra for coagulated flocs were observed. Only three obvious Gaussian peaks were obtained in the C 1s spectra of PACl-C and PACl-Al_{13} flocs, as seen in Fig. 6(b) and (c), where the peak at 283.8 eV, 284.2 eV and 287.6 eV are assigned to aromatic carbon, aliphatic carbon and ketonic carbon, respectively. In this study, the chemical shift of these signals was rather high probably due to pronounced electron withdrawing effect (Szabó et al., 2006). It was also found that the aromatic carbon and aliphatic carbon are two major components among the functional groups of HA before coagulation, but much more aromatic carbon was observed in the coagulated flocs, as listed in Table 2. Other previous study suggested that the aromatic groups preferentially complex with Al_{13} at the optimum coagulant dosage in the acidic range (Kazpard et al., 2006). As a result, the hydrolyzed Al species could favor reactions with aromatic groups

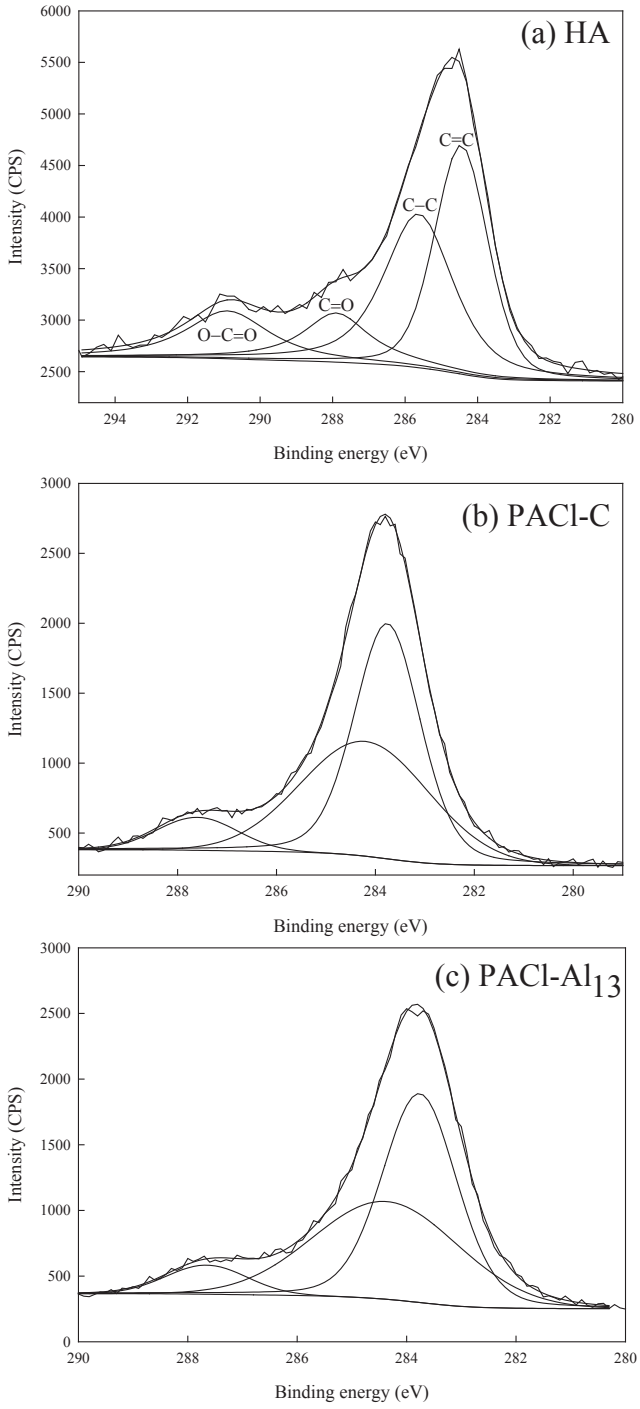

Fig. 6 – C 1s spectra of XPS (a) HA (b)PACl-C flocs (c)PACl-Al_{13} flocs

for optimizing HA destabilization in coagulation at the acidic condition.

3.4. *Mechanism of HA destabilization by PACl-C and PACl-Al_{13} coagulation*

For the optimum HA destabilization by PACl-C and PACl-Al_{13} coagulation at pH 6, the mechanism of HA destabilization by hydrolyzed Al species can be interpreted as shown in Fig. 7.

Table 2 – Surface carbon species of HA and Al–HA flocs.

Peak	Assignment	BE (eV)	Ratio of total carbon (%)
HA			
1	Aromatic C=C	284.5	36.4
2	Aliphatic C–C	285.6	36.1
3	C=O	287.9	12.9
4	O–C=O	290.9	14.6
PACl-C flocs			
1	Aromatic C=C	283.8	50.1
2	Aliphatic C–C	284.2	42.3
3	C=O	287.6	7.6
PACl-Al_{13} flocs			
1	Aromatic C=C	283.8	50.6
2	Aliphatic C–C	284.3	42.4
3	C=O	287.6	7.0

For PACl-C coagulation, the interaction between hydrolyzed Al and HA could be influenced in the presence of sulfate ion. As shown in Fig. 7 (a), because PACl-C coagulation favors sweep flocculation, the majority of colloidal $Al(OH)_3$ formed *in situ* can destabilize HA by adsorption through rapid mixing, and then these $Al(OH)_3$ colloids covered with HA aggregate to form $Al(OH)_3$-HA cluster during flocculation. In part, a low quantity of Al^{3+} binding with SO_4^{2-} to first complex with HA through rapid mixing and then form linear shape precipitates through intermolecular bridging induced by Al^{3+}–SO_4^{2-}–Al^{3+} coordination during flocculation. On the opposite, the majority of Al_{13} polycations containing many binding sites complex with HA by charge neutralization through rapid mixing and then form curled precipitates by intermolecular multidentate complexation during flocculation, as illustrated in Fig 7 (b).

4. Conclusion

For humic acid (HA) destabilization by PACl coagulation at acidic condition, predominant mechanisms for PACl-C coagulation are $Al(OH)_3$-HA co-precipitation, while mechanisms for PACl-Al_{13} coagulation favors charge neutralization and complexation with HA. Therefore, more dosage is required to achieve the optimal HA removal by coprecipitation for PACl-C coagulation than that by complexation for PACl-Al_{13} coagulation. At optimum dosage, larger precipitates with clustered and linear shape have been found within PACl-C flocs in the presence of sulfate ions during coagulation, while smaller curled precipitates have been observed within PACl-Al_{13} flocs due to the formation of intermolecular complex. Monomeric Al substantially undergoes hydrolysis and transforms into $Al(OH)_3$ but remains tetrahedral structure within flocs for PACl-C coagulation in the presence of HA, whereas only a half of Al_{13} is decomposed into octahedral Al–HA precipitates for PACl-Al_{13} coagulation probably due to delayed rate of Al_{13} decomposition. The aromatic groups of HA preferentially react with hydrolyzed Al species for PACl-C and PACl-Al_{13} coagulation. It concludes that the fate of hydrolyzed Al in PACl coagulation for optimizing HA destabilization is governed by the reaction pathway for Al hydrolysis and the interaction between Al and aromatic groups of HA.

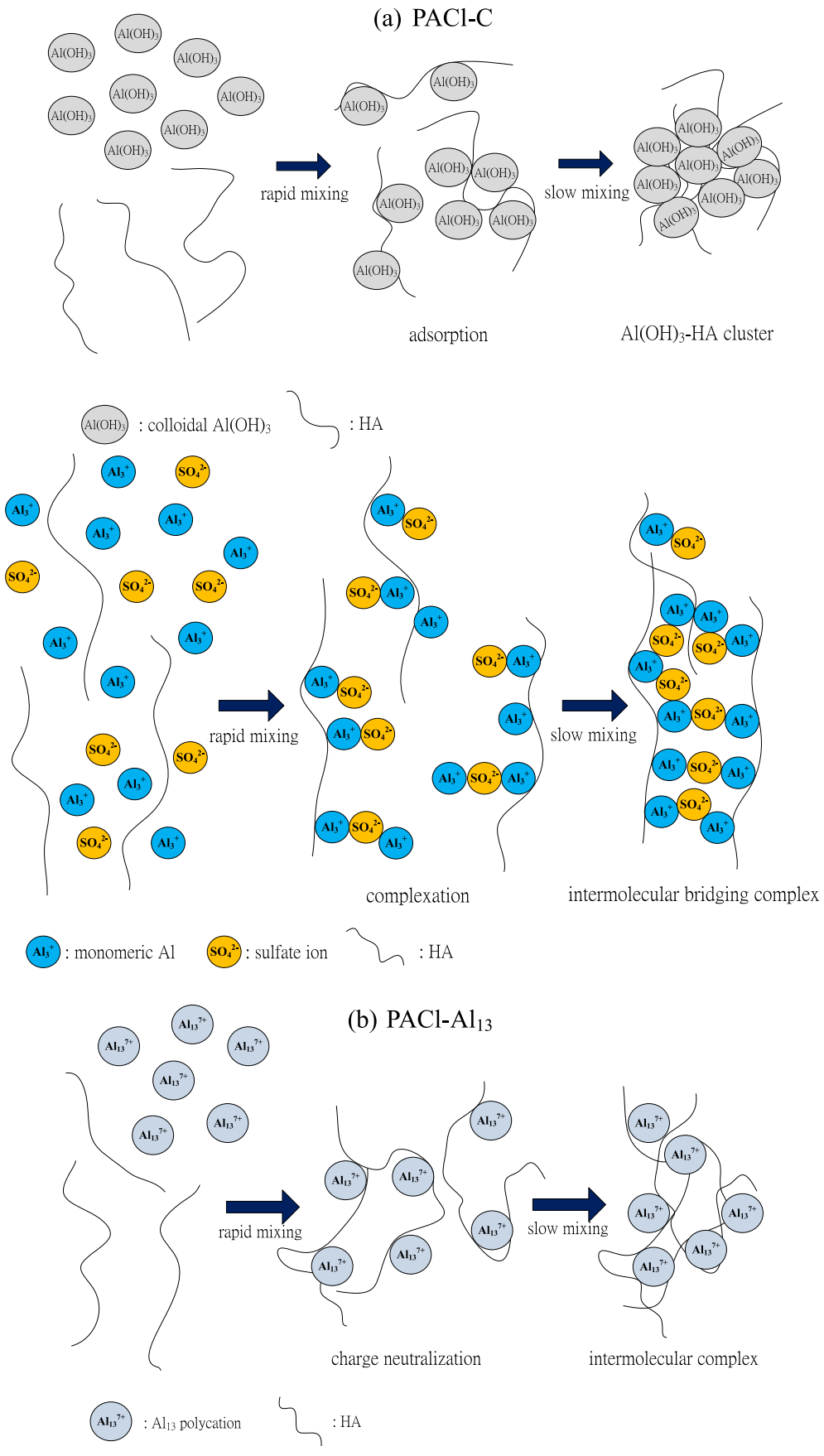

Fig. 7 – Proposed mechanisms of HA destabilization by PACl-C and PACl-Al_{13} coagulation at pH 6.

Acknowledgment

This research was supported by the grant of National Science Council, Taiwan, ROC (NSC 98-2221-E-009-069-MY3). The authors are also grateful to Ms. Chia-hsuan Shih for her kind assistance in analyzing XPS spectra.

REFERENCES

Alborzfar, M., Jonsson, G., Gron, C., 1998. Removal of natural organic matter from two types of humic ground waters by nanofiltration. Water Res. 32 (10), 2983–2994.

Amirbahman, A., Gfeller, M., Furrer, G., 2000. Kinetics and mechanism of ligand-promoted decomposition of the Keggin Al_{13} polymer. Geochim. Cosmochim. Acta 64, 911–919.

Bottero, J.Y., Cases, J.M., Fiessinger, F., Poirier, J.E., 1980. Studies of hydrolyzed aluminum chloride solutions. I. Nature of aluminum species and composition of aqueous solutions. J. Phys. Chem. 84, 2933–2939.

Casey, W.H., 2006. Large aqueous aluminum hydroxide molecules. Chem. Rev. 106 (1), 1–16.

Dempsey, B.A., 2006. Interface Science in Drinking Water Treatment: Theory and Applications (Chapter 2). Academic Press, pp. 5–24.

Dempsey, B.A., Ganho, R.M., O'Melia, C.R., 1984. The coagulation of humic substances by means of aluminum salts. J. Am. Water Works Assoc. 76 (4), 141–150.

Duan, J., Gregory, J., 2003. Coagulation by hydrolyzing metal salts. Adv. Colloid Interface Sci. 100–102, 475–502.

Duong, L.V., Wood, B.J., Kloprogge, J.T., 2005. XPS study of basic aluminum sulphate and basic aluminium nitrate. Mater. Lett. 59 (14–15), 1932–1936.

Edzwald, J.K., Tobiason, J.E., 1999. Enhanced coagulation: US requirements and a broader view. Water Sci. Technol. 40 (9), 63–70.

Exall, K.N., Vanloon, G.W., 2000. Using coagulants to remove organic matter. J. Am. Water Works Assoc. 92 (11), 93–102.

Furrer, G., Phillips, B., Ulrich, K.U., Pöthig, R., Casey, W.H., 2002. The origin of aluminum flocs in polluted streams. Science 297, 2245–2247.

Gallard, H., Gunten, U.V., 2002. Chlorination of natural organic matter: kinetic of chlorination and of THM formation. Water Res. 36 (1), 65–74.

Hiradate, S., Yamaguchi, N.U., 2003. Chemical species of Al reacting with soil humic acids. J. Inorg. Biochem. 97, 26–31.

Hu, C.Z., Liu, H.J., Qu, J.H., Wang, D.S., Ru, J., 2006. Coagulation behavior of aluminum salts in eutrophic water: significance of Al_{13} species and pH control. Environ. Sci. Technol. 40, 325–331.

Huang, C.P., Shiu, H.L., 1996. Interactions between alum and organics in coagulation. Coll. Surf. Physicochem. Eng. Aspects 113, 155–163.

Isobe, T., Watanabe, T., d'Espinose de la Caillerie, J.B., Legrand, A.P., Massiot, D., 2003. Solid-state H-1 and Al-27 NMR studies of amorphous aluminum hydroxides. J. Coll. Interf. Sci. 261 (2), 320–324.

Jin, C.J., Shackelford, C.D., Reardon, K.F., 2008. Association of humic acid with metal (hydr)oxide-coated sands at solid-water interfaces. J. Coll. Interf. Sci. 317, 424–433.

Johansson, G., 1960. On the crystal structures of some basic aluminum salts. Acta Chem. Scand. 14, 771–773.

Kazpard, V., Lartiges, B.S., Frochot, C., d'Espinose de la Caillerie, J.B., Viriot, M.L., Portal, J.M., Gorner, T., Bersillon, J.L., 2006. Fate of coagulant species and conformational effects during the aggregation of a model of a humic substance with Al_{13} polycations. Water Res. 40 (10), 1965–1974.

Lin, J.L., Chin, C.J.M., Huang, C.P., Pan, J.R., Wang, D.S., 2008a. Coagulation behavior of Al_{13} aggregates. Water Res. 42 (16), 4281–4290.

Lin, J.L., Huang, C.P., Chin, C.J.M., Pan, J.R., 2008b. Coagulation dynamics of fractal flocs induced by enmeshment and electrostatic patch mechanisms. Water Res. 42 (17), 4457–4466.

Lin, J.L., Huang, C.P., Chin, C.J.M., Pan, J.R., 2009. The origin of $Al(OH)_3$-rich and Al_{13}-aggregate flocs composition in PACl coagulation. Water Res. 43 (17), 4285–4295.

Liu, H.J., Hu, C.Z., Zhao, H., Qu, J.H., 2009. Coagulation of humic acid by PACl with high content of Al-13: the role of aluminum speciation. Sep. Purif. Technol. 70 (2), 225–230.

Lu, X.Q., Chen, Z.L., Yang, X.H., 1999. Spectroscopic study of aluminium speciation in removing humic substances by Al coagulation. Water Res. 33 (15), 3271–3280.

Masion, A., Vilge-Ritter, A., Rose, J., Stone, W.E.E., Teppen, B.J., Rybacki, D., Bottero, J.Y., 2000. Coagulation-flocculation of natural organic matter with Al salts: speciation and structure of the aggregates. Environ. Sci. Technol. 34 (15), 3242–3246.

Monteil-Rivera, F., Brouwer, E.B., Masset, S., Deslandes, Y., Dumonceau, J., 2000. Combination of X-ray photoelectron and solid-state ^{13}C nuclear magnetic resonance spectroscopy in the structural characterization of humic acids. Anal. Chim. Acta 424, 243–255.

O'Melia, C.R., Becker, W.C., Au, K.K., 1999. Removal of humic substances by coagulation. Water Sci. Technol. 40, 47–54.

Ross, D.S., Bartlett, R.J., Zhang, H., 2001. Photochemically induced formation of the "Al_{13}" tridecameric polycation in the presence of Fe(II) and organic acids. Chemosphere 44, 827–832.

Shen, Y.H., Dempsey, B.A., 1998. Synthesis and speciation of polyaluminum chloride for water treatment. Environ. Int. 24 (8), 899–910.

Sieliechi, J.M., Lartiges, B.S., Kayem, G.J., Hupont, S., Frochot, C., Thieme, J., Ghanbaja, J., Caillerie, J.B.D., Barres, O., Kamga, R., Levitz, P., Michot, L.J., 2008. Changes in humic acid conformation during coagulation with ferric chloride: implications for drinking water treatment. Water Res. 42 (8–9), 2111–2123.

Shi, B.Y., Li, G.H., Wang, D.S., Tang, H.X., 2007. Separation of Al_{13} from polyaluminum chloride by sulfate precipitation and nitrate metathesis. Sep. Purif. Technol. 54, 88–95.

Sposito, G.E., 1996. The Environmental Chemistry of Aluminium, second ed. CRC Press, Inc.

Szabó, T., Berkesi, O., Forgó, P., Josepovits, K., Sanakis, Y., Petridis, D., Dékány, I., 2006. Evolution of surface functional groups in a series of progressively oxidized graphite oxides. Chem. Mater. 18 (11), 2740–2749.

Thomas, F., Masion, A., Bottero, J.Y., Rouiller, J., Montigny, F., Genevrier, F., 1993. Aluminum(III) speciation with hydroxy carboxylic acids. Aluminum-27 NMR study. Environ. Sci. Technol. 27, 2511–2516.

Van Benschoten, J.E., Edzwald, J.K., 1990. Chemical aspect of coagulation using aluminum salts-I: hydrolytic reactions of alum and polyaluminum chloride. Water Res. 24, 1519–1526.

Wang, D.S., Tang, H.X., Gregory, J., 2002. Relative importance of charge-neutralization and precipitation during coagulation with IPF-PACl: effect of sulfate. Environ. Sci. Technol. 36 (8), 1815–1820.

Wang, Y.L., Du, B.Y., Liu, J., 2007. Surface analysis of cryofixation-vacuum-freeze-dried polyaluminum chloride-humic acid (PACl-HA) flocs. J. Coll. Interf. Sci. 316 (2), 457–466.

Wu, Z., Zhang, P., Zeng, G.M., Jiang, J.H., 2012. Humic acid removal from water with polyaluminum coagulants: effect of sulfate on aluminum polymerization. J. Environ. Eng. 138, 293–298.

Xu, W.Y., Gao, B.Y., Wang, Y., Yue, Q.Y., Ren, H.J., 2012. Effect of second coagulant addition on coagulation efficiency, floc properties and residual Al for humic acid treatment by Al-13 polymer and polyaluminum chloride (PACl). J. Hazard. Mater. 215, 129–137.

Yamaguchi, N., Hiradate, S., Mizoguchi, M., 2004. Disappearance of aluminum tridecamer from hydroxyaluminum solution in the presence of humic acid. Soil. Sci. Soc. Am. J. 68 (6), 1838–1843.

Zhao, H., Liu, H.J., Hu, C.Z., Qu, J.H., 2009. Effect of aluminum speciation and structure characterization on preferential removal of disinfection byproduct precursors by aluminum hydroxide coagulation. Environ. Sci. Technol. 43, 5067–5072.

Zhao, H., Hu, C.Z., Liu, H.J., Zhao, X., Qu, J.H., 2008. Role of aluminum speciation in the removal of disinfection byproduct precursors by a coagulation process. Environ. Sci. Technol. 42, 5752–5758.